

# Room temperature continuous wave operation of single-mode, edge-emitting photonic crystal Bragg lasers

Lin Zhu\*, Xiankai Sun, Guy A. DeRose, Axel Scherer and Amnon Yariv

Department of Electrical Engineering and Department of Applied Physics, California Institute of Technology  
Pasadena, California 91125  
[linz@caltech.edu](mailto:linz@caltech.edu)

**Abstract:** We report the first room temperature CW operation of two dimensional single-mode edge-emitting photonic crystal Bragg lasers. Single-mode lasing with single-lobed, diffraction limited far-fields is obtained for 100 $\mu$ m wide and 550 $\mu$ m long on-chip devices. We also demonstrate the tuning of the lasing wavelength by changing the transverse lattice constant of the photonic crystal. This enables a fine wavelength tuning sensitivity (change of the lasing wavelength/ change of the lattice constant) of 0.072. This dependence proves that the lasing mode is selected by the photonic crystal lattice.

©2008 Optical Society of America

**OCIS codes:** (140.5960) Semiconductor lasers; (350.2770) Gratings

---

## References and links

1. S. Wang and S. Sheem, "Two-dimensional distributed-feedback lasers and their applications," *Appl. Phys. Lett.* **22**, 460-462 (1973).
  2. M. Imada, S. Noda, A. Chutinan, T. Tokuda, M. Murata, and G. Sasaki, "Coherent two dimensional lasing action in surface-emitting laser with triangular lattice photonic crystal structure," *Appl. Phys. Lett.* **75**, 316-318 (1999).
  3. S. Noda, M. Yokoyama, M. Imada, A. Chutinan and M. Mochizuki, "Polarization mode control of two-dimensional photonic crystal laser by unit cell structure design," *Science* **293**, 1123-1125 (2001).
  4. D. Ohnishi, T. Okano, M. Imada, and S. Noda, "Room temperature continuous wave operation of a surface-emitting two-dimensional photonic crystal diode laser," *Opt. Express* **12**, 1562-1568 (2004).
  5. M. Meier, A. Mekis, A. Dodabalapur, A. Timko, R. E. Slusher, J. D. Joannopoulos and O. Nalamasu, "Laser action from two dimensional distributed feedback in photonic crystals," *Appl. Phys. Lett.* **74**, 7-9 (1999).
  6. I. Vurgaftman and J. R. Meyer, "Photonic-crystal distributed-feedback lasers," *Appl. Phys. Lett.* **78**, 1475-1477 (2001).
  7. C. S. Kim, W. W. Bewley, C. L. Canedy, I. Vurgaftman, M. Kim, and J. R. Meyer, "Broad-stripe near-diffraction-limited mid-infrared laser with a second order photonic crystal distributed feedback grating," *IEEE Photon. Technol. Lett.* **16**, 1250-1252 (2004).
  8. R. J. Lang, K. D. Zurko, A. Hardy, S. Demars, A. Schoenfelder, and D. Welch, "Theory of grating-confined broad-area lasers," *IEEE J. Quantum Electron.* **34**, 2196-2210 (1998).
  9. L. Zhu, G. A. DeRose, A. Scherer, and A. Yariv, "Electrically-pumped, edge-emitting photonic crystal lasers with angled facets," *Opt. Lett.* **32**, 1256-1258 (2007).
  10. H. Hofmann, H. Scherer, S. Deubert, M. Kamp, and A. Forchel, "Spectral and spatial single mode emission from a photonic crystal distribution feedback laser," *Appl. Phys. Lett.* **90**, 121135 (2007).
  11. L. Zhu, X. K. Sun, G. A. DeRose, A. Scherer, and A. Yariv, "Continuous-wave operation of electrically-pumped, single-mode, edge-emitting photonic crystal Bragg lasers," *Appl. Phys. Lett.* **90**, 261116 (2007).
  12. K. Paschke, A. Bogatov, F. Bugge, A. E. Drakin, J. Fricke, R. Guther, A. A. Stratoniuk, H. Wenzel, and G. Erbert, "Properties of ion-implanted high-power angled-grating distributed-feedback lasers," *IEEE J. Sel. Top Quantum Electron.* **9**, 1172-1178 (2003).
  13. L. Zhu, P. Chak, J. K. S. Poon, G. A. DeRose, A. Yariv, and A. Scherer, "Electrically-pumped, broad-area, single-mode photonic crystal lasers," *Opt. Express* **15**, 5966-5975 (2007).
  14. L. A. Coldren and S. W. Corzine, *Diode Lasers and Photonic Integrated Circuits*, (Wiley Interscience, 1995).
  15. D. Botez and D. R. Scifres, *Diode Laser Arrays* (Cambridge University Press, 1986).
-

## 1. Introduction

The idea of using two dimensional distributed feedback in lasers dates back to 1973 [1]. Two dimensional distributed feedback lasers, also named as photonic crystal Bragg lasers, select the lasing mode using the Bragg reflection from a two dimensional weak index perturbation. Spatial coherence over a large area can be obtained, allowing for potential single-mode, high power operation with small beam divergence. In this letter, we report the first room temperature continuous wave (CW) operation of two dimensional distributed feedback, single-mode, edge-emitting semiconductor lasers.

There are two basic design approaches to two dimensional distributed feedback structures: surface-emitting and edge-emitting [2-7]. For surface-emitting lasers, light has to satisfy the Bragg conditions to diffract out of the plane. Two dimensional distributed feedback surface-emitting lasers have been demonstrated in both semiconductor and polymer materials. Room temperature CW operation has also been obtained for a  $50\mu\text{m} \times 50\mu\text{m}$  single-mode surface-emitting laser [4]. For edge-emitting lasers, the design has to incorporate discrimination mechanisms against gain-guided modes, which prevent the single-mode operation of large-area, edge-emitting semiconductor lasers [8]. Photonic crystal distributed feedback structures with angled facets have been proposed to overcome this problem [6]. So far, single-mode operation of large-area, edge-emitting semiconductor lasers using two dimensional distributed feedback has only been demonstrated either in room temperature pulsed condition [9, 10] or low temperature CW condition [11].

Here we report the first room temperature CW operation of two dimensional single-mode edge-emitting photonic crystal Bragg lasers. These lasers break the limit of the index guiding for designing edge-emitting, single-mode semiconductor lasers using distributed feedback structures. This work constitutes the most critical step toward broad-area, single-mode, high beam quality, high power semiconductor lasers with multiple available wavelengths. Our lasers are about  $100\mu\text{m}$  wide and  $550\mu\text{m}$  long. We measure the light-current (L-I) curve, spectrum, near-field and far-field of the laser. Despite the non-uniform intensity distribution in the near-field, the far-field is single-lobed and diffraction-limited. This proves that the photonic crystal Bragg structure can prevent filamentation and ensure a single-mode operation. We also demonstrate tuning of the lasing wavelength by changing the transverse lattice constant of the photonic crystal. This enables a fine wavelength tuning sensitivity (change of the lasing wavelength/ change of the lattice constant) of 0.072. This dependence also proves that the lasing mode is selected by the photonic crystal lattice.

## 2. Design and fabrication of photonic crystal Bragg lasers

Figure 1 shows a schematic diagram of a typical photonic crystal Bragg laser and the wafer structure. The surface photonic crystal consists of a rectangular lattice array of polymer-filled holes. The angled facets are used to suppress gain-guided modes [6-8]. In the wafer plane, an optical mode that satisfies both transverse and longitudinal Bragg resonance conditions will be confined due to the distributed Bragg reflection. Outside the metal contact region, the lasers are implanted with protons to confine the current distribution and prevent unwanted sidelobes in the far-field [12]. Figure 2 shows scanning electron microscope (SEM) images of the fabricated devices. The fabrication details can be found in Ref. [13].

We use a first order Bragg reflection for the transverse direction with a lattice constant of  $a = 1.04\mu\text{m}$  and a second order Bragg reflection for the longitudinal direction with a lattice constant of  $b = 490\text{nm}$ . The design corresponds to a resonance wavelength of  $1553\text{nm}$  (The effective index  $n_{\text{eff}}$  is estimated to be 3.257). The hole radius is  $100\text{nm}$  and the etch depth is about  $400\text{nm}$ . The metal contact width is  $100\mu\text{m}$  and the tilt angle is  $13.8^\circ$ . The design details are discussed in Ref. [9]. The lasers are cleaved to lengths of about  $550\mu\text{m}$  and are P-side up

bonded to a C-mount using indium solder. The C-mount is then screwed on a thermoelectric cooling (TEC) stage and the temperature is set at 13°C.

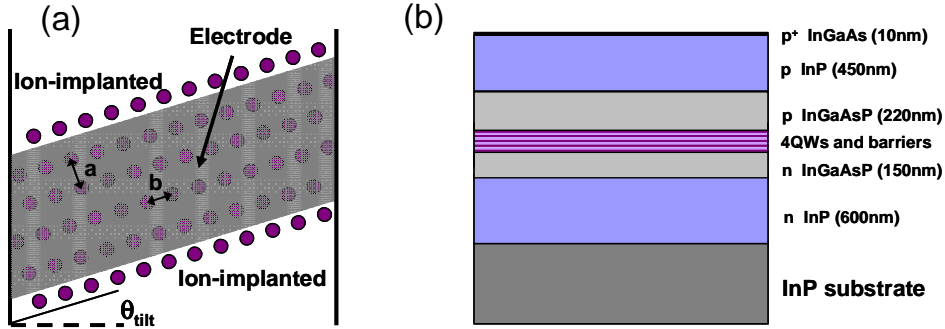


Fig. 1. Device design and wafer structure. (a) Schematic of a two dimensional photonic crystal Bragg laser.  $a$  is the transverse lattice constant,  $b$  is the longitudinal lattice constant, and  $\theta_{\text{tilt}}$  is the facet tilt angle. (b) Epitaxial structures of the material used to fabricate the lasers. The design uses a standard graded-index separate confinement heterostructure.

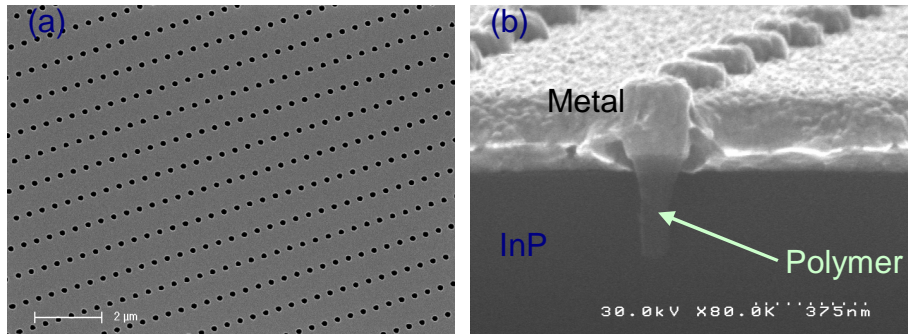


Fig. 2. SEM images of the fabricated devices. (a) Overall view of the photonic crystal lattice. The image is taken after the etch of InP. (b) The cross section of a fabricated PC Bragg laser with top metal contacts. Each etched hole is filled with planarization polymer.

### 3. Experiment results and discussions

Single-mode CW operation of these lasers has been obtained. Figure 3(a) shows the photonic crystal Bragg laser characteristics of the output power versus the input current (L-I) and the voltage versus the input current (I-V). In the I-V curve, the turn-on voltage of 0.75V is much lower compared to our previous devices (~1.5V) since we make the planarization polymer slightly higher than the wafer surface. In this case, the metal layer will not be in the direct contact with the etched semiconductor. In the L-I curve, the laser has a clear threshold at 560mA. The device can be operated up to ~2.5x threshold and further increase of the pumping current leads to thermal rollover. The slope efficiency is 0.08W/A, which is similar to the broad area lasers fabricated from the same wafer under the same test conditions. This indicates that this efficiency is mainly limited by the wafer material and the thermal management. Although p-side down bonding provides much better thermal performance, we use p-side up bonding since the metal contacts are relatively thin (~250nm). Figure 3(b) shows the emission spectrum at an injection current of 1.2A. The single-mode operation is obtained with the side mode suppression ratio (SMSR) higher than 30dB. The laser also maintains the single-mode operation under different pumping currents.

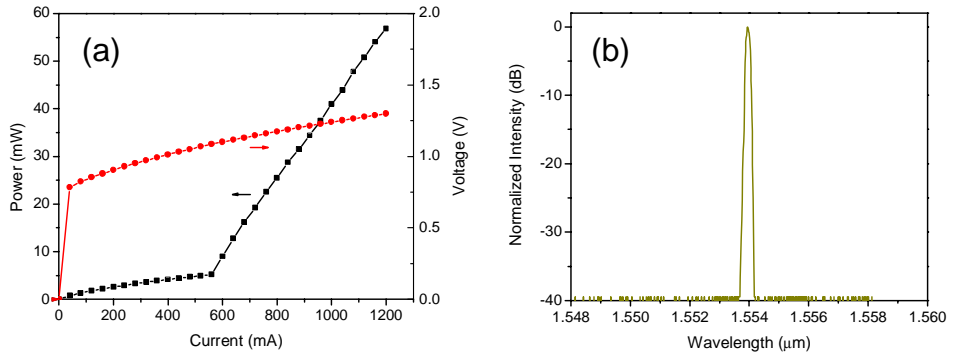


Fig. 3. (a). L-I and I-V curves for the photonic crystal Bragg laser. The turn-on voltage is 0.75V and the resistance is  $0.68\Omega$ . The threshold is 560mA. (b). The emission spectrum at the injection current  $I=1.2A$

The photonic crystal Bragg laser by limiting operation to a single transverse mode prevents filamentation, which leads to spatial coherence over the large emitting aperture. This results in a single-lobe diffraction-limited far field with small beam divergence. Figure 4 shows the near-field and far-field profiles of the test laser when the pumping current is 1.2A. As shown in Fig. 4(a), the laser has a multi-lobe near-field. This is mainly due to the material gain non-uniformity over a large width (100μm). This kind of non-uniformity generally leads to filamentation for a typical broad area laser or a ridge waveguide laser, resulting in multi-lobe far fields and big beam divergence [14]. However, the far-field of the photonic crystal Bragg laser is single-lobed and possesses a small beam divergence angle of  $1^\circ$ , as shown in Fig. 4(b). (In the CCD far-field image, the fringes in the vertical direction are due to unwanted interferences in the measurement.) The emitting aperture of the laser is about 100μm, corresponding to a theoretical diffraction-limited far-field FWHM (full width at half maximum) width of  $0.99^\circ$  [15]. This shows that the photonic crystal Bragg laser can operate in a single-lobe diffraction-limited far-field.

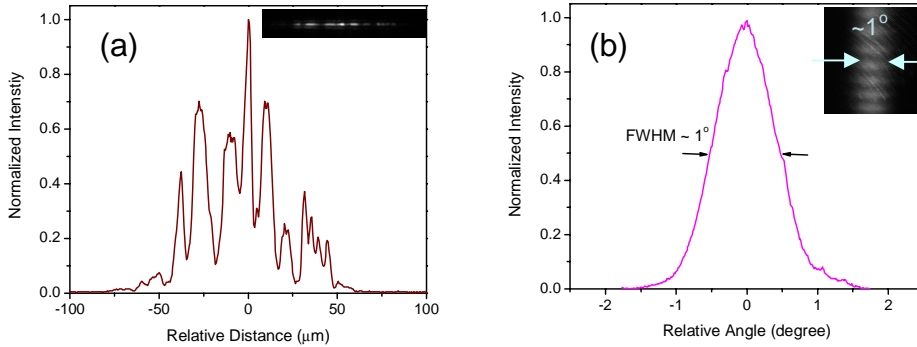


Fig. 4. (a). Near field and (b) far field profiles of the photonic crystal Bragg laser ( $I=1.2A$ ). The insets are direct images captured by infrared CCD cameras.

Transverse and longitudinal Bragg conditions need to be satisfied simultaneously in our lasers since the lasing mode is confined by the photonic crystal lattice. This enables us to tune the lasing wavelength by changing either the longitudinal or the transverse lattice constant. In our design, the transverse Bragg wavevector is much smaller than the longitudinal Bragg wavevector. This results in the ability to finely tune the lasing wavelength with a relatively large step of the transverse lattice constant. To show this advantage, we fabricate the lasers with the same longitudinal constant of  $b = 490\text{nm}$  and four different transverse lattice

constants of  $a = 0.96\mu\text{m}$ ,  $1.0\mu\text{m}$ ,  $1.04\mu\text{m}$ , and  $1.08\mu\text{m}$  on the same chip. Figure 5 shows the lasing spectra at  $\sim 1.1 \times$  threshold for all the four lasers. The measured laser wavelengths ( $1546.9\text{nm}$ ,  $1550.3\text{nm}$ ,  $1552.8\text{nm}$  and  $1555.6\text{nm}$ ) are close to the theoretical predictions ( $1546.2\text{nm}$ ,  $1549.9\text{nm}$ ,  $1553.2\text{nm}$  and  $1556.2\text{nm}$ ) calculated from the Bragg conditions (see Ref. [9] for more details about the theoretical lasing wavelength calculations). As the transverse lattice constant changes from  $0.96\mu\text{m}$  to  $1.08\mu\text{m}$ , the lasing wavelength shifts  $8.6\text{nm}$ . This corresponds to a transverse tuning sensitivity of 0.072, about thirty times smaller than a typical DFB laser. This small tuning sensitivity can provide accurate control of the lasing wavelength.

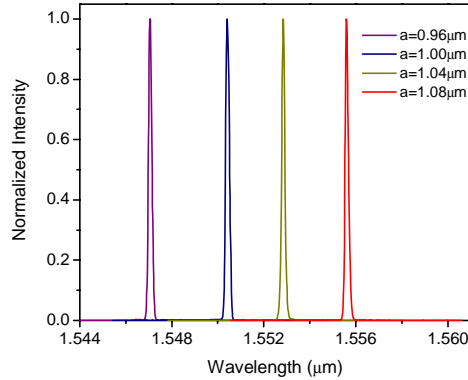


Fig. 5. Lasing spectra at  $\sim 1.1 \times$  threshold. These four lasers have the same longitudinal lattice constant  $b = 490\text{nm}$  but different transverse lattice constants  $a = 0.96\mu\text{m}$ ,  $1.0\mu\text{m}$ ,  $1.04\mu\text{m}$ , and  $1.08\mu\text{m}$ . The measured laser wavelengths are  $1546.9\text{nm}$ ,  $1550.3\text{nm}$ ,  $1552.8\text{nm}$  and  $1555.6\text{nm}$ . A small tuning sensitivity of 0.072 is obtained.

#### 4. Conclusion

In summary, we have demonstrated electrically-pumped, large-area, edge-emitting photonic crystal lasers in InGaAsP active semiconductor materials operating at room temperature under CW condition. Single-mode lasing with single-lobed, diffraction limited far-fields is obtained for  $100\mu\text{m}$  wide and  $550\mu\text{m}$  long devices. In order to prove that the lasing mode is defined by the photonic crystal, we finely tune the lasing wavelength by changing the transverse lattice constant and achieve a tuning sensitivity of 0.072. These results demonstrate that photonic crystal Bragg lasers are good candidates for broad-area, single-mode, high beam quality, high power semiconductor lasers.

#### Acknowledgments

The authors thank Dr. P. Chak, Dr. J. Choi, and Dr. J. Poon for helpful discussions. This work was supported by the subaward from ONR under Contract No. N00014-05-M-0254.